ELSEVIER

Journal of Non-Crystalline Solids 296 (2001) 158–164

JOURNAL OF NON-CRYSTALLINE SOLIDS

www.elsevier.com/locate/jnoncrysol

Effects of heat treatment and concentration on the luminescence properties of erbium-doped silica sol–gel films

L.H. Slooff [a,1], M.J.A. de Dood [a], A. van Blaaderen [a,b], A. Polman [a,*]

[a] *FOM Institute for Atomic and Molecular Physics, Kruislaan 407, 1098 SJ Amsterdam, Netherlands*
[b] *Condensed Matter Department, Debye Institute, Utrecht University, P.O. Box 80000, 3508 TA Utrecht, Netherlands*

Received 14 November 2000; received in revised form 20 August 2001

Abstract

Erbium-doped sol–gel films with different Er concentrations were formed by spin-coating a solution of erbium-nitrate, tetra-ethoxy-silane (TEOS), ethanol, water and HCl on a Si substrate. Refractive index, film thickness and composition were measured as a function of Er concentration. The Er/Si ratio in the film is roughly proportional to the Er/Si ratio in solution, while the Si/O ratio varies with the Er concentration. The film thickness increases with increasing Er concentration, which is attributed to the increased viscosity of the spin-coat solution compared to pure SiO_2. All films show a lower refractive index and atomic density than pure SiO_2, which is ascribed to a slightly porous structure. After annealing at 750 °C in vacuum the films show clear room-temperature luminescence at 1.53 μm from Er^{3+}. The luminescence lifetime is rather constant (10–12 ms) up to Er concentrations of 1.0 at.%. The luminescence lifetime reduces significantly if annealing is performed in air rather than in vacuum.

1. Introduction

Er-doped silica glass materials are finding more and more applications in photonic technology. For example, Er-doped fibers are used as the gain medium in long-distance optical fiber links, operating at 1.53 μm. Er-doped silica channel waveguides find applications in planar optical amplifiers that are used in photonic integrated circuits [1], and Er-doped colloidal silica particles might be integrated with polymer technology to fabricate nano-composite waveguide materials [2]. As the quantum efficiency of the luminescent Er transition at 1.53 μm can be quite high, Er-doped silica could also find applications in photonic crystals, as a probe of the local optical density of states [3].

Several methods have been developed to fabricate Er-doped silica, including plasma-enhanced chemical–vapor-deposition [4], ion implantation [5], flame hydrolysis [6], and ion exchange [7]. An alternative technique to deposit thin Er-doped silica films is by using a wet chemical process, in which a solution containing a silica precursor and erbium-nitrate is spin-coated on a substrate,

* Corresponding author. Tel.: +31-20 608 1234; fax: +31-20 668 4106.
E-mail address: polman@amolf.nl (A. Polman).
[1] Present address: ECN Solar Energy, Thin Film PV Technology, PO Box 1, 1755 7G Petter, The Netherlands.

0022-3093/01/$ - see front matter
PII: S0022-3093(01)00903-6

followed by a drying step (the sol–gel process). The advantage of this technique is that many different constituents can be added to the solution in order to tailor the film composition, refractive index, and Er solubility. Besides this, the spin-coat technique makes it possible to use virtually any substrate.

Quite some research has been done on Er-doped sol–gel films [8–14]. In most cases, composite silica-based materials were studied, or bulk glasses were made rather than thin films, but only a few focus on pure silica sol–gel films. In this paper we report on a systematic study of the effect of Er concentration on the film stoichiometry, thickness, atomic density and refractive index for silica films with Er concentrations in the range 0.05–1.0 at.%. Luminescence spectra and lifetime are studied versus Er concentration. We find that the luminescence lifetime depends critically on the annealing ambient. Films annealed in vacuum show lifetimes as high as 11 ms, a factor of 3 higher than that reported for pure Er-doped sol–gel films so far.

2. Experiment

Er-doped sol–gel films (set I) were prepared in the following way. First a tetra-ethoxy-silane (TEOS) reaction mixture was made: 23.0 g TEOS (Fluka 99%), 5.0 g ethanol (pro analysi, Merck), 5.9 g H_2O and 2.2 g 0.1 M HCl (Aldrich) were mixed, and then stirred while heated to a temperature of 70 °C, at which it was kept for 5 min. After stirring for 3 min, the solution changed from opaque to transparent. An Er solution was prepared by dissolving 3.1 g of $Er(NO_3)_3 \cdot 5H_2O$ (Aldrich 99.9%) into 10.0 ml ethanol. Solutions with different Er concentrations were made by adding 0.05, 0.1, 0.3, 0.6, and 1.0 ml of the Er solution to 7.0 ml of the TEOS reaction mixture. In order to have a similar ethanol concentration in the different reaction mixtures, the volume of all solutions was made equal to 8.0 ml by adding ethanol. Each solution was left to react for 4.5 h and then spin-coated onto pre-cleaned Si substrates, covered by a $\sim$2 nm thick native oxide. Spin-coating was performed at 3500 rpm for 60 s. After spin-coating the samples were dried at 60 °C for 10 min in air.

To study the effect of annealing ambient on the luminescence lifetime, two additional sets of samples (set II and III) were prepared using a slightly different ratio of the chemicals compared to set I, in order to obtain a better spinable solution. A mixture of 4.8 g TEOS, 1.1 g ethanol, 0.4 g H_2O and 0.5 g 0.1 M HCl, together with a solution of 0.29 g $Er(NO_3)_3 \cdot 5H_2O$, was dissolved into 1 ml ethanol. After the same reaction period as mentioned above, the solution was spin-coated at 2000–4000 rpm, followed by a heat treatment of 60 °C for 10 min in air.

Sets I and II were annealed for 1 h in vacuum (10^{-6} mbar) at 100 °C, followed by 1 h at 900 °C (set I) or 750 °C (set II). Set III was annealed in air rather than vacuum at the same temperatures as set II.

Erbium depth profiles and film stoichiometry were measured by Rutherford backscattering spectrometry (RBS) using 2 MeV He^+ ions at a backscattering angle of 165°. Layer thickness and refractive index were measured using spectroscopic ellipsometry at incedent angles of 55°, 60°, 65°, 70° and 75° relative to the surface normal. The wavelength was scanned from 300 to 1700 nm in 5 nm steps.

Photoluminescence (PL) measurements were performed using the 488 and 515 nm lines of an Ar-ion laser as an excitation source operating at a power of 30 or 100 mW. The emitted luminescence was projected onto the entrance slits of a 48 cm monochromator and detected with a liquid-nitrogen-cooled Ge detector. Standard lock-in techniques were employed, using a mechanical chopper to modulate the laser beam. The spectral resolution was 2–6 nm. Photoluminescence lifetime measurements were performed by monitoring the decay of the luminescence after switching off the light source. A digitizing oscilloscope was used to average the decay curves. The time response of the system was about 30 μs. An optical microscope was used to study the surface morphology of the sol–gel layers.

3. Results

RBS spectra of the Er-doped sol–gel layers of set I (before annealing) are shown in Fig. 1 for

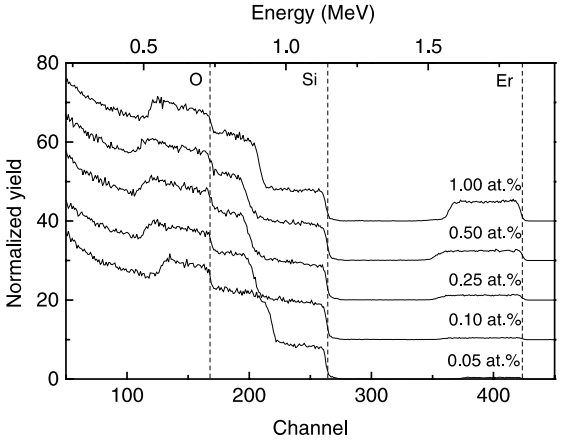

Fig. 1. RBS spectra for Er-doped sol–gel films before annealing (set I). Data are shown for concentrations ranging from 0.05 to 1.0 at.%. Spectra are offset for clarity. Surface channels for O, Si and Er are indicated.

different Er concentrations. Surface channels for the elements O, Si and Er are indicated by dashed lines. The Si surface channel is observed around channel 260, corresponding to the Si in the SiO_2 film. The edge at channel 210 shows the interface between the Si substrate and the SiO_2 film. The plateau below channel 165 relates to the oxygen in the SiO_2 layer. The width of this plateau varies for the different Er concentrations, indicating differences in the layer thickness. The SiO_2 coverage derived from the width of these plateaus agrees with that derived from the width of the plateaus around channel 400, which shows the erbium distribution in the film. From the ratio of erbium-nitrate to TEOS in the reaction solution, an estimate of the Er atomic concentration in each film can be made, assuming a stoichiometric SiO_2 film composition. These estimates are shown in Table 1 for set I together with the film compositions as derived from fits to the RBS spectra (fits not shown). As can be seen, the Er concentrations in the film are quite similar to the estimated values. In fact, the Er/Si ratio in the film is similar to the Er/Si ratio in the solution. This makes it possible to tailor the Er concentration rather accurately. Table 1 also shows the film areal density for all five layers as derived from RBS. As can be seen, the areal density and film composition are slightly different for the five Er concentrations. The layer with the highest Er concentration has an almost pure SiO_2 stoichiometry, while the other layers are somewhat Si-rich.

The thickness of the spin-coated layers of set I (before annealing), as measured by ellipsometry, is plotted in Fig. 2 versus the nominal Er concentration derived from the Er/Si ratio in solution. All measurements were performed in the center of the sample. As can be seen, the layer thickness increases with increasing Er concentration. This was also observed by Bruynooghe et al. [14] and was attributed to an increase in the initial solution viscosity for increasing Er concentration. Using the measured film thickness, the areal density from Table 1 can be converted into an atomic density, which is also shown in Table 1. The resulting atomic density is in the range $(4.1–5.5) \times 10^{22}$ cm^{-3}, which is lower than that for pure SiO_2 (6.6×10^{22} cm^{-3}). Fig. 3 shows the refractive index for these samples as a function of wavelength (set I) as obtained from ellipsometry measurements. The refractive index increases with increasing Er concentration, but stays well below that for thermally grown SiO_2 that is also shown in

Table 1
Er concentration estimated from the Er/Si ratio in the solution together with the areal density and layer composition of Er-doped sol–gel films derived from RBS measurements

Er concentration from Er/Si ratio in solution (at.%)	Film composition (at.%)			Film areal density (10^{15} atoms/cm^2)	Atomic density (cm^{-3})
	Si	O	Er		
1.05	35	64	1.00	3000	4.1×10^{22}
0.63	45	55	0.50	3400	5.0×10^{22}
0.32	45	55	0.25	3400	5.1×10^{22}
0.11	45	55	0.10	3400	5.4×10^{22}
0.05	40	60	0.05	2500	4.6×10^{22}

The atomic density is derived from the areal density data together with the thickness measurements from ellipsometry.

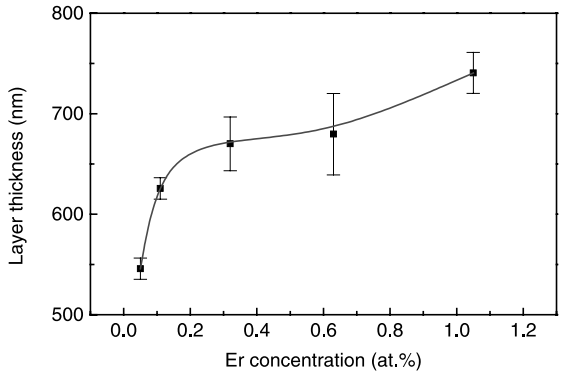

Fig. 2. Layer thickness of the spin-coated Er-doped layers before annealing (set I) versus Er concentration, as derived from spectroscopic ellipsometry measurements.

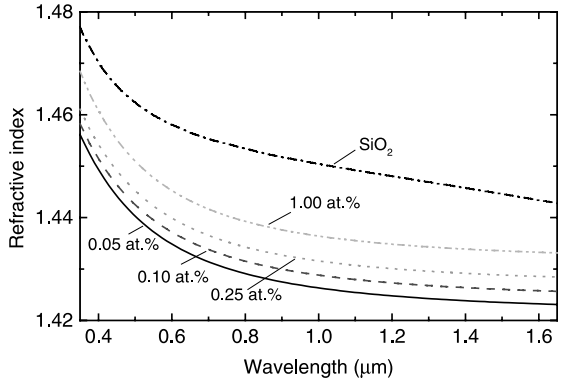

Fig. 3. Refractive index as a function of wavelength for spin-coated films doped with different Er concentrations (before annealing). Data for thermally grown pure SiO_2 are also shown.

Fig. 3 [15]. This, together with the fact that all films are relatively Si-rich (which would increase their refractive index compared to that of stoichiometric SiO_2), and the lower atomic density compared to pure SiO_2, leads to the conclusion that the spin-coated materials have a porous structure before annealing.

Fig. 4 shows a normalized PL spectrum of a 1.0 at.% Er-doped sol–gel film of set I, after annealing at 900 °C in vacuum for 1 h. The spectrum was taken using an excitation wavelength of 488 nm at a pump power of 30 mW. The Er^{3+} luminescence around 1.53 μm is clearly visible and results from the intra-4f transition from the

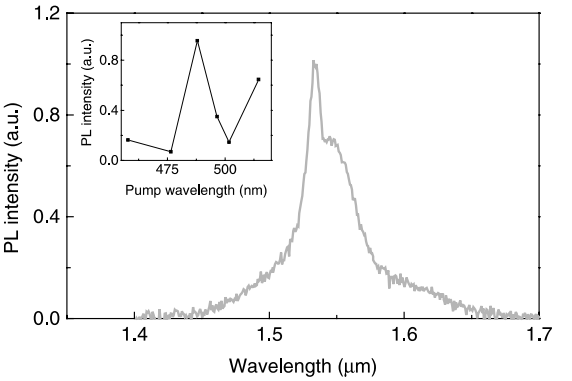

Fig. 4. Photoluminescence spectrum of a 1.0 at.% Er-doped film (set I) annealed at 900 °C in vacuum. The excitation wavelength was 488 nm at a pump power of 30 mW. The inset shows a photoluminescence excitation spectrum of the 1.53 μm emission intensity.

first excited state ($^4I_{13/2}$) to the ground state ($^4I_{15/2}$). The inset of Fig. 4 shows the 1.53 μm luminescence intensity as a function of excitation wavelength for the same sample. This spectrum reflects the structure of the optical absorption bands from the ground state ($^4I_{15/2}$) to the $^4F_{7/2}$ state (490 nm) and the $^2H_{11/2}$ state (514 nm), showing that the Er^{3+} ions in these SiO_2 layers are excited through direct optical excitation. This is well known for Er^{3+} in insulating materials [16], in contrast to the case of Er in Si-rich oxide materials like e.g. amorphous Si/SiO_2 [17] or Si nanocrystal-doped SiO_2 [18,19] in which the Er^{3+} excitation is photocarrier-mediated.

We have tried to measure the PL intensity as a function of the Er concentration. Cracking of the films after annealing resulted in a strong scattering of the laser light, making comparison of the absolute intensities difficult. However, in general the intensity increases for increasing concentration. An optical microscope image of a pure sol–gel film without Er annealed in vacuum at 900 °C for 1 h is shown in Fig. 5. One can observe 'jig-saw-puzzle'-like pieces that clearly fit together, indicating that the cracks are the result of shrinkage [20]. It is well known that sol–gel films of several hundred nm thickness crack during annealing when water and organic residues evaporate from the film. It is also known that growing thinner layers and repeating

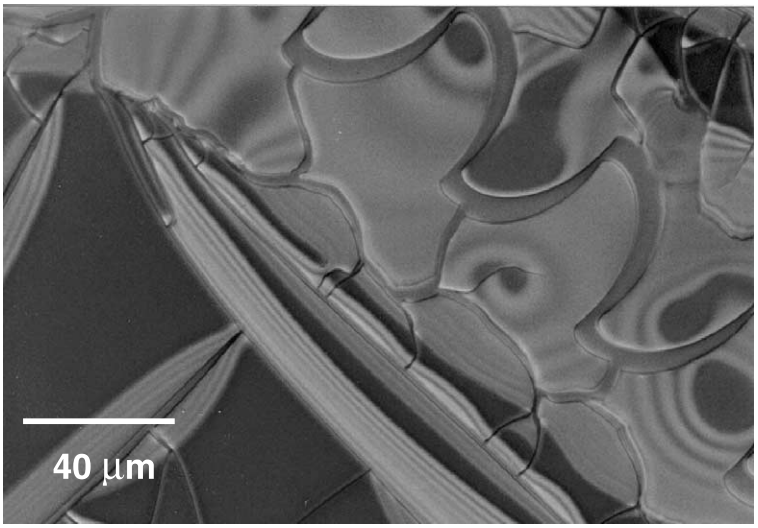

Fig. 5. Optical microscope image of a vacuum-annealed (900 °C, 1 h) pure sol–gel film without Er. Cracks due to shrinkage of the film are clearly seen.

the spin-coat-drying step several times can overcome this problem [21].

The luminescence lifetimes for different Er concentrations are shown in Fig. 6 for the films of set I (samples annealed in vacuum at 900 °C). For Er concentrations up to 1.0 at.%, the luminescence lifetime remains more or less constant at 10–12 ms. Often, in highly Er-doped materials, the luminescence lifetime is seen to decrease with concentration due to quenching by OH impurities

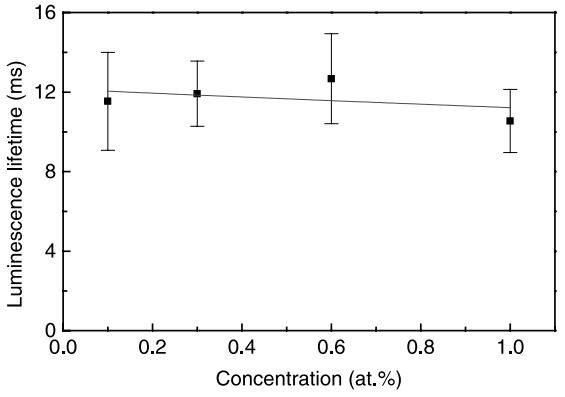

Fig. 6. Luminescence lifetime for spin-coated sol–gel films annealed in vacuum (set I) as a function of Er concentration. The excitation wavelength was 515 nm at a pump power of 30 mW. The drawn line is a guide to the eye.

(the second overtone of the O–H stretch vibration is resonant with the Er transition at 1.53 μm) [22–26]. An effect that becomes apparent at high Er concentrations, when Er–Er energy migration takes place. The fact that we measure long luminescence lifetimes at high Er concentration thus indicates that most of the water is removed from the film during the anneal treatment. By taking a simple linear concentration quenching model, and assuming a typical Er–Er coupling constant of 10^{-51} m^6/s, we can estimate from the data in Fig. 6 the O–H concentration to be ~18 ppm. Note that this analysis is based on the assumption that Er does not precipitate after annealing, an effect that would reduce the amount of optically active Er. This assumption is supported by the observed increase in the luminescence intensity with Er concentration. Transmission electron microscopy was performed to verify this, and although some dark spots with a size of several nm were visible, these could not be identified as being Er-rich. More work is necessary to verify this point.

The luminescence lifetimes in Fig. 6 are much longer than the lifetime of 1.78 ms reported by Orignac et al. [13] for similar Er-doped sol–gel films. One of the main differences between that work and the samples described here is the fact

that our films were annealed in vacuum, whereas the films by Orignac et al. were annealed in air. To study the effect of the annealing ambient, we prepared two new sets of 1.0 at.% Er-doped silica films: one set was annealed at 750 °C in vacuum (set II) and the other set in air (set III). Fig. 7 shows PL decay traces for the two films. Clearly the air-annealed sample has a shorter lifetime (7.7 ms) than the vacuum-annealed sample (10.5 ms). A possible explanation is that in the case of an anneal in air more O–H remains in the film compared to the case of an anneal in vacuum, which might be due to a slower release of physically and chemically absorbed water. More research is needed to verify this. However, there still remains a large difference between the lifetime measured in this paper and the work of Orignac et al. Based on a linear quenching model, the amount of quencher (in this case the OH concentration [OH]) can be calculated

$$W = W_r + W_i + 8\pi C_{Er\text{–}Er}[Er][OH], \quad (1)$$

where W_r is the radiative lifetime ($\sim 55\ s^{-1}$) [27], W_i the internal non-radiative decay rate, $C_{Er\text{–}Er}$ ($\sim 10^{-51}\ m^6/s$) a coupling constant, and [Er] is the Er concentration. This results in an OH concentration of $4.1 \times 10^{18}\ cm^{-3}$ for the present Er concentration of $4 \times 10^{20}\ cm^{-3}$ for the anneal in vacuum, and an OH concentration of $7.6 \times 10^{18}\ cm^{-3}$ for the anneal in air. In the case of Orignac et al. the Er concentration is slightly lower ($2.6 \times 10^{20}\ cm^{-3}$). Using Eq. (1), this results in an OH concentration of $7.7 \times 10^{19}\ cm^{-3}$. This OH concentration is about 10 times higher than that for our air annealed samples. This higher OH concentration might be explained by the fact that Orignac et al. use a H_2O/TEOS ratio of 4, where we used a ratio of 1. This means that four times more water is present in the films of Orignac et al. resulting in an eight times higher OH concentration. Besides this, there is also a difference in anneal temperature which could affect the amount of H_2O in the film.

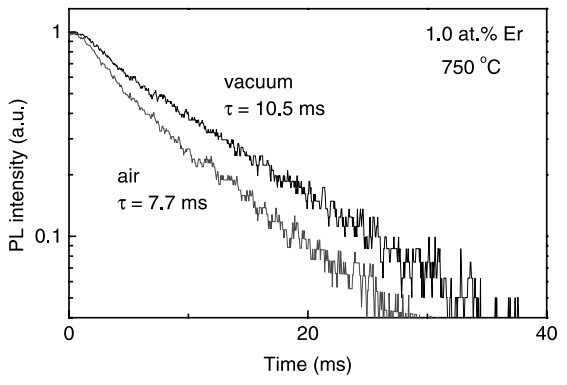

Fig. 7. Luminescence decay traces ($\lambda = 1.53$ μm) for 1.0 at.% Er^{3+}-doped sol–gel films, annealed at 750 °C in vacuum (set II) or air (set III). The excitation wavelength was 515 nm at a pump power of 100 mW.

4. Conclusions

Er-doped silica films were prepared by spin-coating a solution of erbium- nitrate, tetra-ethoxy-silane, ethanol, water and HCl on a Si substrate. Film thickness (550–750 nm) and composition vary slightly with Er concentration in the range 0.05–1.0 at.%. The refractive index and atomic density of all films is lower than those of pure SiO_2, indicating that the films are porous. After annealing at 900 °C, room temperature photoluminescence at 1.53 μm is observed with a luminescence lifetime as long as 10–12 ms, for Er concentration up to 1.0 at.%. Using a concentration quenching model we conclude that most of the water is removed from the film during the anneal treatment; the O–H content is estimated to be below 1 ppm. Anneals were also performed in air and led to shorter lifetimes, possibly caused by a higher O–H content. Our measurements show that the sol–gel process in combination with vacuum annealing is ideally suited to obtain Er-doped silica exhibiting long luminescence lifetimes.

Acknowledgements

This work is part of the research program of the foundation for Fundamental Research on Matter (FOM) and was financially supported by the Dutch Foundation for Scientific Research (NWO) and the SCOOP program of the European Union.

Daniël Sentenac is gratefully acknowledged for assisting with spin-coating of the films.

References

[1] see for a review P.G. Kik, A. Polman, MRS Bull. 23 (1998) 48.
[2] L.H. Slooff, M.J.A. de Dood, A. van Blaaderen, A. Polman, Appl. Phys. Lett. 76 (2000) 3682.
[3] E. Snoeks, A. Lagendijk, A. Polman, Phys. Rev. Lett. 74 (1995) 2459.
[4] K. Shuto, K. Hattori, T. Kitagawa, Y. Ohmori, M. Horiguchi, Electron. Lett. 29 (1993) 139.
[5] A. Polman, J. Appl. Phys. 82 (1997) 1.
[6] T. Kitagawa, K. Hattori, K. Shuto, M. Yasu, M. Kobayashi, M. Horiguchi, Electron. Lett. 28 (1992) 1818.
[7] T. Feuchter, E.K. Mwarania, J. Wang, L. Reekie, J.S. Wilkinson, IEEE Photo Tech. Lett. 4 (1992) 542.
[8] C.K. Ryu, H. Choi, K. Kim, Appl. Phys. Lett. 66 (1995) 2496.
[9] X. Fan, M. Wang, G. Xiong, Mater. Lett. 27 (1996) 177.
[10] B.T. Stone, K.L. Bray, J. Non-Cryst. Solids 197 (1996) 136.
[11] Y. Kurokawa, T. Ishizaka, T. Ikoma, S. Tero-Kubota, Chem. Phys. Lett. 287 (1998) 737.
[12] M. Benatsou, B. Capoen, M. Bouazaouni, W. Tchana, J.P. Vilcot, Appl. Phys. Lett. 71 (1997) 428.
[13] X. Orignac, A. Barbier, X.M. Xu, R.M. Almeida, Appl. Phys. Lett. 69 (1996) 895.
[14] S. Bruynooghe, A. Chabli, F. Bertin, F. Pierre, J. Mater. Res. 12 (1997) 2779.
[15] E.D. Palik, in: Handbook of Optical Constants in Solids I, Academic Press, New York, 1985.
[16] V. Dierolf, M. Koerdt, Phys. Rev. B. 61 (2000) 8043.
[17] S. Lombardo, S.U. Campisano, G.N. van den Hoven, A. Cacciato, A. Polman, Appl. Phys. Lett. 63 (1993) 1942.
[18] P.G. Kik, M.L. Brongersma, A. Polman, Appl. Phys. Lett. 76 (2000) 2325.
[19] M. Fujii, M. Yoshida, Y. Kanzawa, S. Hayashi, K. Yamamoto, Appl. Phys. Lett. 71 (1997) 1198.
[20] L.C. Klein, Ann. Rev. Mater. Sci. 15 (1985) 227.
[21] A.S. Holmes, R.R.A. Syms, M. Li, M. Green, Appl. Opt. 32 (1993) 4916.
[22] V.P. Gapontsev, A.A. Izyneev, Yu.E. Sverchov, M.R. Syrtlanov, Sov. J. Quantum Electron. 11 (1981) 1101.
[23] E. Snoeks, P.G. Kik, A. Polman, Opt. Mater. 5 (1996) 159.
[24] A.J. Bruce, W.A. Reed, A.E. Neeves, L.R. Copeland, W.H. Grodkiewicz, A. Lidgard, Mater. Res. Soc. Symp. Proc. 244 (1992) 157.
[25] Y. Yan, A.J. Faber, H. de Waal, J. Non-Cryst. Solids 181 (1995) 283.
[26] F. Auzel, in: B. DiBartolo (Ed.), Radiationless Processes, Plenum, New York, 1980.
[27] M.J.A. de Dood, L.H. Slooff, A. Moroz, A. van Blaaderen, A. Polman, Phys. Rev. A 64 (2001).